Confinement Effect on the Effective Viscosity of Plasticized Polymer Films

F. Chen,[1] D. Peng,[1] Y. Ogata,[2] K. Tanaka,[2] Z. Yang,[3] Y. Fujii,[4] N. L. Yamada,[5] C. -H. Lam,[6*] and O. K. C. Tsui[1,7]*

[1]*Department of Physics, Boston University, Boston, MA 02215.*

[2]*Department of Applied Chemistry, Kyushu University, Fukuoka 819-0395, Japan*

[3] *Department of Polymer Science and Engineering, Soochow University, P. R. China*

[4] *National Institute for Materials Science, 1-1 Namiki, Tsukuba, Japan.*

[5] *Neutron Science Laboratory, High Energy Accelerator Research Organization, Ibaraki 305-0044, Japan.*

[6] *Department of Applied Physics, Hong Kong Polytechnic University, Hung Hom, Hong Kong.*

[7] *Division of Materials Science & Engineering, Boston University, Brookline, MA 02446.*

ABSTRACT: We have measured the effective viscosity of polystyrene films with a small (4 wt%) added amount of dioctyl phthalate (DOP) deposited on silica. A broad range of molecular weights, M_w, from 13.7 to 2,100 kg/mol was investigated. Our result shows that for the thin films with M_w < ~100 kg/mol, the addition of DOP causes the effective viscosity to decrease by a factor of ~4, independent of M_w. But for the higher M_w films, the effective viscosity of the DOP added films creeps towards that of the neat films with increasing M_w. A model assuming the effective viscosity to be dominated by enhanced surface mobility for the lower M_w films, but surface-promoted interfacial slippage for the higher M_w films is able to account for the experimental observations.

INTRODUCTION

Many experiments in the past two decades have witnessed significant changes to the glass transition temperature, T_g, and related dynamics of a polymer when the polymer is cast into thin films with thicknesses, h_0, less than ~100 nm.[1, 2] For polymer films supported by a solid substrate, most results showed that the strength of the polymer-substrate interaction dictates whether the T_g increases or decreases with decreasing film thickness although new factors were discovered more recently. A brief account of the present state of affairs follows. Typically, strong, attractive interactions lead to T_g enlargement while weakly attractive or neutral interactions lead to T_g reduction.[3, 4] An example of the former is atatic polymethyl methacrylate (PMMA) supported by silica (SiOx).[5, 6] The T_g enlargement of this system is commonly attributed to the strong hydrogen bonding that can form between the carbonyl group on the side chains of the polymer and the hydroxyl groups on the substrate surface. [7] Conversely, for polystyrene (PS) supported by SiOx -- an example demonstrating T_g reduction, [4, 8-10] the interactions between the polymer and substrate surface are weak. [7] The milder effect expected of the substrate surface may then be marginalized by the effect of the free surface, where enhanced polymer mobility was observed in most polymers, [11-14] and found to be able to facilitate T_g reduction. [15] Comparable manners by which different interfaces modify the dynamics of a polymer film are also observed in computer simulations.[15, 16] Theoretical models [17-21] constructed upon akin interfacial effects were able to demonstrate agreement with experiment. More recently, it was found that the interfacial free volume found in an out-of-equilibrium polymer layer adsorbing onto the solid substrate can also influence a

film's T_g. [22, 23] Polymer films, placed above or sandwiched within another layer of immiscible polymer also exhibited variations in the T_g. [24] These observations were demonstrated to be consistent with a kinetic lattice model of free volume and mobility transport accounting for the interfacial mobility profile at the free surface of a fluid or interface between two fluids. [25]

About a decade ago, Torkelson et al. investigated the effect of plasticizer addition on the T_g of a variety of polymer films, including poly(vinyl acetate) (PVAc) supported by glass,[26] PS supported by glass (PS-SiOx),[9] and poly(2-vinyl pyridine) and PMMA supported by quartz (P2VP-SiOx and PMMA-SiOx, respectively). [5] These workers found that plasticizer addition generally causes the thickness dependence of the T_g to weaken or even disappear. The magnitude of this effect depends on the specific system considered and the amount of plasticizer used. Torkelson et al. explained their observations by a connection between the size scale of the cooperative dynamics associated with glass transition (which decreases with plasticizer addition) and the size scale of the T_g confinement effect, which they estimated to be over ~30 nm.[27]

More recently, Nguyen et al. [28] studied the effect of confinement on the dynamics of PVAc deposited separately on aluminum and gold upon plasticization by water uptake at different relative humidity. Their T_g measurement displayed thickness independence and so possible consistency with the result of Torkelson et al.. The effect of water uptake on the dynamics of PVAc and PMMA films was also investigated by other groups and generally found to produce enhanced dynamics.[29, 30] But because the amount of water taken in by the films was not known, it was not possible to conclude if the T_g confinement effect observed by Torkelson et al. may translate into analogous effects (i.e.,

thickness independence) on other measures of dynamics in plasticized polymer films. It was also not possible to elicit by what way confinement may or may not modify these dynamic measures.

In this experiment, we investigate the effective viscosity, η_{eff}, of PS-SiOx films plasticized with 4 wt% of dioctyl phthalate (DOP). Unlike the reported T_g of this system, [9] we find that η_{eff} of these films decreases noticeably with decreasing film thickness, demonstrating the effect of confinement on η_{eff} to be different than that on T_g for these films. By using a model basing on the interfacial effects previously established for PS-SiOx neat films [31] – namely enhanced mobility at the free surface and surface-promoted interfacial slippage – while at the same time allowing for segregation effects of the DOP to the interfaces, we are able to account for the data well.

EXPERIMENTAL METHODS

Materials Polystyrene (PS) homopolymers with various weight average molecular weights, M_w between 13.7 and 2,100 kg/mol and polydispersity index, PDI, of 1.01 to 1.1, are purchased from Scientific Polymer Products (Ontario, NY), and used without purification. According to the supplier, one end of the polymer is a butyl group and the other end is saturated styrene. Dioctyl phthalate (DOP) is purchased from Sigma-Aldrich, and used here as the plasticizer at a fixed concentration of 4 wt%. Deuterated DOP (dDOP) is purchased from Kanto Chemical Co., INC. (Tokyo, Japan) for studying the distribution of DOP in the films by neutron reflectivity (NR). According to the literature, DOP has a solubility parameter of 8.9 $(cal/cm^3)^{0.5}$,[32] which is comparable to that of PS (= 9.1 $(cal/cm^3)^{0.5}$),[33] and reportedly a theta θ solvent of PS near room temperature.[34]

Film Preparation Method To make the films, the PS polymer with or without the plasticizer is first dissolved in toluene. Then the solution is filtered through a PTFE membrane filter with pore size 0.1 μm (Fisher Scientific Co.) before spin-cast onto the substrate, namely single crystal (001) silicon covered by a 102 ± 5 nm thick thermal oxide (Siltronix, France). Before use, the substrates are cleaned in a piranha solution (H_2SO_4 : H_2O_2 = 7:3) at 130 ^oC for 10 min. Afterward, they are thoroughly rinsed with deionized water and then dried with 99.99% nitrogen. This is followed by final cleansing in oxygen plasma for 20 min. The thickness of the polymer film is measured by ellipsometry at 5 different locations of the film. Deviations found in the measured thickness are less than 0.3 nm.

Neutron Reflectivity **(**NR) is used to determine the DOP profile in the films. Measurements are carried out at ambience on the plasticized PS films containing 4 wt% deuterated DOP (dDOP) with M_w = 60.5 (thickness, h_0 = 11 nm) and 1,400 kg/mol (h_0 = 13 nm). NR profiles were collected at the Soft Interface Analyzer (SOFIA) (BL-16, Materials and Life Science Facility, Japan Proton Accelerator Research Complex, Tokai, Japan), which is a horizontal-type reflectometer.[35, 36] A neutron beam with a wavelength (λ) ranging from 0.25 to 0.88 nm at a resolution of 3% was guided onto the film from the air side. The incident angles of the beam were set to 0.3, 0.7 and 1.8°. The analyses of the profiles were carried out using the Parratt32 software based on Parratt's algorithm. The (b/V) values for PS, dDOP, SiOx and Si used in these calculations were taken as 1.42 × 10^{-4}, 6.70 × 10^{-4}, 4.15 × 10^{-4} and 2.08 × 10^{-4} nm^{-2}, respectively.

Irreversibly adsorbed layer thickness measurement is used to assess the relative polymer-substrate interaction strength between samples. To prepare the irreversibly

adsorbed polymer layers, PS-SiOx (neat or DOP-added) with a thickness of 200 nm are fabricated as described above. Then the films are annealed at 150 ^{o}C for 80 h. Afterward they are rinsed in copious amounts of toluene and submerged in a beaker of 100 mL toluene for 10 min. This process is repeated two more times. Ellipsometry is used to estimate the thickness of the irreversibly adsorbed polymer layer remaining on the substrate. Measurements are performed at 10 different locations of each sample. The mean and standard deviation is taken to be the thickness measurement and uncertainty, respectively. The measured irreversibly adsorbed layer thicknesses of neat PS-SiOx are consistent with what we found before. [37]

Bulk Viscosity Measurement Dynamic mechanical analysis (DMA) is used to determine the bulk viscosity of the polymers with $M_w \geq 60.5$ kg/mol at temperature T = 182 ^{o}C (c.f. the boiling point of DOP is 384 ^{o}C). The measurements are performed on a strain-controlled AR2000 Rheometer (TA Instruments, New Castle, DE) operated in the oscillation test mode (with $0.5 \leq \omega \leq 500$ rad/s) with 20 mm parallel plates. The strain is fixed at (2 ± 0.3) %, and checked to lie within the linear viscoelastic response regime. The samples are molded in a vacuum press for 30 min. and then loaded to the rheometer at room temperature. The gap between the parallel plates is adjusted to about 1 mm and maintained at the same value during measurement. For data treatment, the Rheology Advantage Data Analysis software is used. For polymers with lower M_w's ($\leq$ 116 kg/mol), we determine the bulk viscosity at T = 120 ^{o}C by studying the surface dynamics of thin films made of these polymers (method described below), where the film thickness is chosen to be sufficiently large that the viscosity measurement exhibits no discernible variation when the film thickness is further increased. The use of different measurement

methods at different temperatures allows the bulk viscosity to be determined for a broad range of M_w.

Thin Film Viscosity Measurement In these measurements, the films are used as-cast without thermal annealing. Because the as-cast films are smoother than equilibrium, they roughen upon heating above the T_g.[38] The surface topography of the films is measured by ex-situ tapping-mode atomic force microscopy (AFM) at various roughening times, t. (This means that AFM measurements are performed on the films upon quenching them to room temperature.) Annealing is carried out under ambient condition. We limit t to be shorter than the time it takes the film's rms roughness to exceed 10% of the average film thickness or deep holes discernible by AFM begins to form. The use of AFM for the detection of holes is necessary here as the films showing deep holes by AFM may still appear smooth by optical microscopy. The above measures assure that linear approximations, to which our analysis is based, are applicable. To prepare the data for modeling, each topographic data is converted to its power spectral density (PSD), $A_q^2(t)$, by following the procedure detailed in Ref. [13]. Figure 1 shows a representative sequence of PSDs we obtained. (Some representative AFM images and the respective rms roughness values are displayed in Figure S2 of the Supplementary Information.) For this data set, the PSD does not evolve with time during the initial ~10 h of annealing (except for the rapid jump in the first time step, which is attributable to the glass-to-rubber transition. [39]) Even though the PSD is stagnant with time, frame-to-frame comparison of the AFM images taken in independent in-situ measurements shows that the surface topography is not. This indicates that the films are in a quasi-steady state,

undergoing equilibrium vibrations. We attribute the vibrations to the normal modes of the films in the rubbery elastic state. At later times, growth of the PSDs resumes.

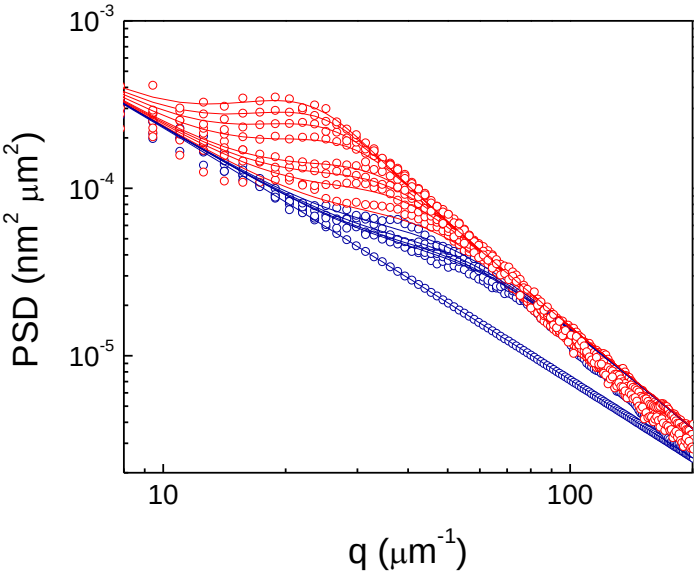

Fig. 1. (Color online) Illustration of a typical set of power spectral density (PSD) we obtain and goodness of the model fit. The data (symbols) shown are collected from a neat PS-SiOx film with thickness, h_0 = 5 nm and M_w = 393 kg/mol at 120 ^oC for times of (from bottom to top) blue: 0, 600, 1200, 2400, 4800, 9600, 24000; red: 36000, 48000, 96000, 144000, 192000 and 253420s. The solid lines are the model fits using eq 1a with η_{eff} = 1.5 × 10^8 Pas and μ_0 = 11.0 kPa. Reprinted with permission from Ref. [31]. Copyright 2015 American Chemical Society.

This shows that there are two dynamic processes with different time scales, associable with the initial stagnant and subsequent PSD growth stages. Adopting an adiabatic approximation, we analyzed the slow evolution in the presence of the ensemble-averaged quasi-equilibrium elastic vibrations. The slow evolution is described by the in-plane transport currents, $\boldsymbol{j}(\boldsymbol{r}, t)$, caused by fluctuations in the local film profile, $h(\boldsymbol{r})$, that in turn produces gradients in the local pressure $P(\boldsymbol{r}, t)$ according to: $\boldsymbol{j}(\boldsymbol{r}, t) = -M_{tot}\nabla P(\boldsymbol{r}, t)$,

where M_{tot} is the mobility of the film. [40] For the fast vibrations, we assume the normal mode energy to be $[3\mu_0/(2h_0^3q^2)]|u_{\mathbf{q}}|^2$, consistent with elastic vibrations with wavevector $\boldsymbol{q}$ and amplitude $u_{\mathbf{q}}$ [41], where $q \equiv |\boldsymbol{q}|$ and μ_0 is the shear modulus of the film. A linear stability calculation assuming lubrication approximation and stable films gives: [40]

$$A_q^2(t) = A_q^2(0)\exp(2\Gamma_q^{'}t) + \left(\frac{k_BT}{\gamma_s q^2 + G''(h_0)}\right)\left(1-\exp(2\Gamma_q^{'}t)\right) \qquad (1a)$$

where $$\Gamma_q^{'} = -M_{tot}q^2\left[\left(\gamma_s q^2 + G''(h_0)\right)^{-1} + \left(\frac{3\mu_0}{h_0^3 q^2}\right)^{-1}\right]^{-1}. \qquad (1b)$$

In the above, k_B is the Boltzmann constant, T is absolute temperature, γ_s is surface tension, and $G(h_0)$ is the van der Waals potential of the films. [42]

For the cases where $\Gamma_q' < 0$, $\lim_{t\to\infty} A_q^2(t) = k_BT/[\gamma q^2 + G''(h_0)]$. Equation 1 may then be written as

$$A_q^2(t) = [A_q^2(0) - A_q^2(\infty)]\exp(2\Gamma_q^{'}t) + A_q^2(\infty). \qquad (2)$$

In this form, we can see that if the initial PSD, $A_q^2(0)$, differs from the equilibrium PSD, $A_q^2(\infty)$, the first term causes their difference to diminish exponentially at a rate constant given by Γ_q'. The last term ensures that $A_q^2(t) = A_q^2(0)$ at $t = 0$. Taken together, eq 1 portrays a dynamic process by which the surface of the film evolves from the initial structure toward equilibrium by means of the surface capillary wave modes with dispersion relation given by eq 1b. The solid lines in Figure 1 display the best fit to eq 1. As seen, the fitted lines agree with experiment well. It should be mentioned that all the

other films also exhibit similar agreement for the whole annealing process. This is an important observation, especially for the films annealed at high temperatures. It is because it indicates that thermal degradation has negligible impact on the measurement, for otherwise the data should show a tendency to evolve faster than predicted at later times corresponding to the viscosity of the film decreasing with time.

If the slow process is caused by viscous shear flow in a film where the viscosity, η, is uniform and there is no interfacial slip, then $M_{tot} = h_0^3/(3\eta)$. We define the effective viscosity (which, being derived from M_{tot}, is associated with the slow process) by: [13, 40]

$$\eta_{eff} \equiv h_0^3/[3M_{tot}]. \qquad (2) \quad (3)$$

Given the definition, if no slippage occurs and the fluid viscosity does not vary with position in the film, η_{eff} would be the same as the fluid viscosity. Otherwise, η_{eff} is an effective viscosity and may exhibit a dependence on h_0 in general.[13, 31] By modeling M_{tot} or η_{eff} to match the observed h_0 dependence, one may infer information about the nature of the slow process.[13, 31]

RESULTS AND DISCUSSIONS

Figure 2 displays the bulk viscosity, η_{bulk}, of the plasticized and neat PS plotted as a function of M_w obtained at T = 120 ^oC and 182 ^oC. Empirically, all the data series can be fitted to the $\eta_{bulk} \sim M_w^{3.2\pm0.2}$ power law. Theoretically, η_{bulk} follows Rouse dynamics or $\sim M_w$ when M_w is smaller than the characteristic molecular weight, M_c ($\approx$ 31 kg/mol for PS [43]), but switches to reptation dynamics $\sim M_w^{3.4}$ when M_w is increased above M_c. Such a crossover for PS is smeared out as seen in Figure 2, attributable to its M_w

dependence of free volume in the lower M_w regime.[44] For the data taken at 120 ^oC, η_{bulk} of the neat polymer is 4.0 ± 0.5 times that of the plasticized polymer. For the data taken at 182 ^oC, a similar multiplying factor, namely 3.5 ± 0.5 is found. In general, addition of plasticizers to a polymer causes its viscosity to decrease. The origin of this effect can be twofold. First, plasticizers possess more free volume and so by mixing them with a

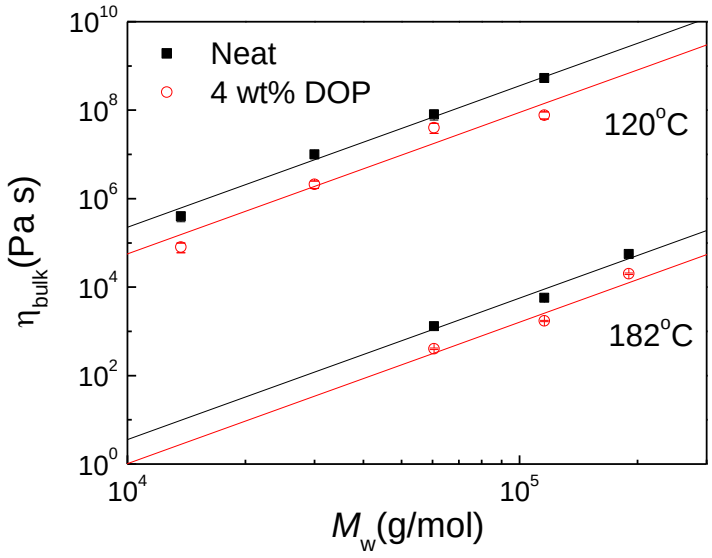

Fig. 2. Plot of bulk viscosity versus M_w obtained from neat PS (solid squares) and DOP-added PS (open circles). The data marked to be taken at 182 ^oC were obtained by using DMA. The data taken at 120 ^oC were determined from the dynamics of surface capillary waves in thick films where further increase in the film thickness did not bring about discernible change to the measurement. The solid lines are fits to the empirical scaling law, $\eta_{bulk} \sim M_w^{3.2\pm0.2}$.

polymer can cause a net increase in the free volume of the system. Secondly, plasticizers often swell the polymer chains resulting in a reduction of the entanglement density. [45] Given these two possibilities, the fact that the ratio of η_{bulk}(neat PS) / η_{bulk}(4wt%DOP-PS)

is, within experimental uncertainty, independent of whether M_w exceeds M_c or not suggests that that the observed viscosity reduction upon DOP addition is primarily caused by free volume augmentation. In fact, the value of the viscosity ratio one finds basing on entanglement density reduction alone, which is predicted to be ~ $\phi^{-3.9}$, [45] is only ~1.2 and so too small to account for the observation (where ϕ is the volume fraction of the added

Table 1. Free Volume Parameters[*] of the 940K PS and DOP

	B/f_0	α_f/B (K^{-1})
PS	15.94	6.17×10^{-4}
DOP	3.91	9.90×10^{-4}

[*]The tabulated data assumes a reference temperature of T_{ref} = 151 °C. Data of PS are based on Ref. [44]. Data of DOP are based on Ref. [46].

DOP, which is about 5 vol% for the 4 wt% used.) According to the free volume theory, [47] an increase in free volume should correspond to a decrease in the monomeric friction coefficient, ξ_0. We estimate the order of magnitude change in ξ_0 due to the free volume change from the added 5 vol% DOP. For this purpose, a reference temperature of T_{ref} = 151 °C, midway between the two measurement temperatures, is assumed. According to the free volume theory, [46, 47]

$$\frac{\xi_0(0)}{\xi_0(\phi)} = \exp\left[\frac{B}{f_0(0)} - \frac{B}{f_0(\phi)}\right], \qquad (3) \quad (4)$$

where B is a constant of order unity, $f_0(\phi)$ is the fraction of free volume in a polymer with plasticizer concentration ϕ (in vol%). Table 1 displays the free volume parameters of PS with M_w = 940 kg/mol [44] and DOP [46] at the reference temperature. (The parameter, α_f, in Table 1 is the thermal expansivity of free volume.) Because B is of the order unity, and the values of α_f/B for PS and DOP differ by less than a factor of two (Table 1), we approximate α_f to be the same for PS and DOP. With this, f_0(DOP)/f_0(PS) $\approx \frac{B/f_0(\text{PS})}{B/f_0(\text{DOP})} \cdot \frac{\alpha_f/B\ (\text{PS})}{\alpha_f/B\ (\text{DOP})}$ = 2.5. Addition of 5 vol% DOP to PS should thus cause f_0 to increase by 5% × (2.5 – 1) = 7.5%. Because B is a constant, this increase in f_0 translates to a decrease of B / f_0 to 15.94 / 1.075 = 14.83. Substituting this estimate of B / f_0 (at ϕ = 5 vol%) and the value of B / f_0 (at ϕ = 0) = 15.94 in eq 3, we obtain $\xi_0(0)/\xi_0(\phi)$ = 3.0. Incorporating the factor 1.2 due to reduction in entanglement density estimated above, we find η_{bulk}(neat PS)/η_{bulk}(DOP-added PS) = 3.6. Considering crudeness of the calculation, this estimate agrees remarkably well with our experimental values. These results support the interpretation that the reduction in viscosity upon DOP addition is primarily caused by a reduction in the monomeric friction coefficient.

Figure 3 displays our main result. It encompasses plots of η_{eff} versus M_w obtained from h_0 = 4 nm thin films of neat (solid symbols) and DOP-added (open symbols) PS-SiOx. At low M_w, the two measurements differ by a constant multiplying factor of about 5. But as M_w exceeds ~100 kg/mol, the difference narrows with increasing M_w. On reaching M_w = 2,100 kg/mol, the two measurements become essentially the same within error bars. Importantly, the convergence is brought about solely by the measurement of

the DOP added films creeping toward that of the neat films. Given that the added DOP modifies η_{eff} chiefly by moderating the polymeric friction, the data of Figure 3 indicates

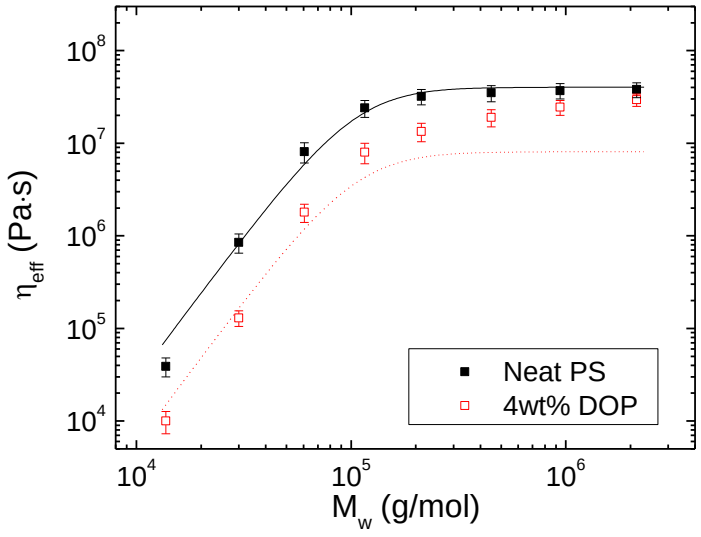

Fig. 3. Viscosity of neat and DOP-added PS-SiOx films with a thickness of 4 nm plotted against M_w. The data were taken at 120 °C. The solid line is a fit of eq 4 to the data of the neat films. The data of the DOP-added films do not fit eq 4. The dotted line is a calculation obtained by dividing the solid line data by 5.

that the relevant friction changes from one source to another as M_w is increased past ~100 kg/mol.

The interpretation that the polymeric friction governing the flow dynamics of polymer nanometer films may change origin with M_w was first introduced in Ref. [31] to account for the observation that η_{eff} of PS-SiOx changes from $\sim M_w^{3.2 \pm 0.2}$ to $\sim M_w^{0}$ with increasing M_w near ~100 kg/mol, which can also be seen in Figure 3. Specifically, it was proposed [31] that the contribution from interfacial slippage to the mobility of a film, M_{tot}, may dominate at high M_w above 100 kg/mol whereupon the polymer-substrate interfacial

friction becomes the dominant source of friction governing the flow dynamics. By solving the Navier-Stokes equation in the lubrication approximation and taking into account enhanced surface mobility and interfacial slippage, one finds: [31]

$$M_{tot} \approx h_0^3/(3\eta_{bulk}) + M_{mobile} + h_0^2/\xi, \quad (4) \quad (5)$$

where M_{mobile} denotes the mobility of a nanometer thin region near the free surface with enhanced mobility relative to the bulk [6, 12-14] and ξ denotes the polymer-substrate interfacial friction. In eq 4, a cross term is neglected for simplicity. The error that may be caused in dropping this term is estimated to be < 20%,[31] which is smaller than the size of the error bars. The last term accounts for interfacial slippage and would be absent if interfacial slippage were negligible.

One may perceive how on physical grounds interfacial slippage can dominate at high M_w as follows. For low-M_w, unentangled polymer films, experiments showed that enhanced surface flow or M_{mobile} dominates M_{tot}. [6, 13, 48, 49] However, as M_w is increased and reaches the point where the perpendicular radius of gyration, $R_\perp$, of the polymer equals the thickness of the surface mobile layer, the surface chains become partially embedded in the slow bulklike inner region and so may no longer sustain enhanced surface flow. At the same time, the contribution to M_{tot} from the inner region of the film, $\approx h_0^3/(3\eta_{bulk})$, [13] diminishes rapidly with decreasing h_0 and increasing M_w (because $\eta_{bulk} \sim M_w^{3.4}$). These make possible for the dominance of M_{tot} by polymer-substrate interfacial slippage, which is normally not observed in PS-SiOx when the film thickness is more

than tens of nanometers (as seen in Figure 6 below). A confinement effect, [31] to be discussed below, also helps promote interfacial slippage.

We have used eq 4 to model the data of the neat films in Figure 3 using ξ as the only fitting parameter. For h_0 and η_{bulk}, we used the experimental and published values, [44] respectively. For M_{mobile}, the relation $M_{mobile} = a_{mobile} M_w^{-3.2}$ was used, with $a_{mobile} = (4.0 \pm 0.2) \times 10^9$ $nm^3Pa^{-1}s^{-1}g^{3.2}mol^{-3.2}$ as determined in Ref. [31] basing on an expansive measurement of η_{eff} on neat PS-SiOx from h_0 = 3 to 20 nm. The fitted value of ξ hence found is $(3.1 \pm 0.5) \times 10^{16}$ Nsm^{-3}, which agrees with the value found before. [31] The result of the fit is displayed by the solid line in Figure 3. Apparently, it describes the data well.

A few words should be said about the relation, M_{mobile} = (constant) $\times M_w^{-3.2}$ assumed above. It was based on the experimental observation that $\eta_{eff} \sim M_w^{3.2\pm0.2}$ in the low M_w regime where M_{mobile} dominated M_{tot}. It is tempting to attribute this scaling as an implication that the dynamics in the surface mobile region follows reptation. However, there are practical issues to consider. First, the thickness of the surface region with enhanced mobility is only 1 to 3 nm,[31, 50] which is significantly smaller than the diameter of an entanglement tube in bulk (c.f. for PS, the tube diameter is ~ 9 nm as approximated by the average end-to-end distance of a polymer chain with $M_w = M_e$. [45]) Secondly, computer simulations[50] showed that the dynamics within the surface region is quite heterogeneous, with the monomeric mobility decreasing rapidly from the free surface at a characteristic distance of about one monomer size. Given these circumstances, it is not obvious how reptation dynamics may take place in the surface mobile region, and whether it may engender the same scaling relation between the local viscosity and M_w as that found in the bulk. Questions as such concerning the nature of the chain dynamics in

the surface region warrant future investigations. It should be mentioned that the first argument may ostensibly challenge the use of the same $\eta_{bulk}(M_w)$ dependence up to high M_w's for thin films with h_0 < 9 nm. But for these films, M_{tot} is already dominated by interfacial slippage, as evident from the $\eta_{eff} \sim M_w^0$ dependence found. Under this circumstance, the precise values of η_{bulk} (and those of M_{mobile} as well) should not affect the accuracy of the model.

We now discuss the data of the plasticized films in Figure 3. As shown by the dotted line, eq 4 is able to describe the data in the M_w < 100 kg/mol regime only. As M_w is increased above 100 kg/mol, the agreement worsens with M_w. For the data in the

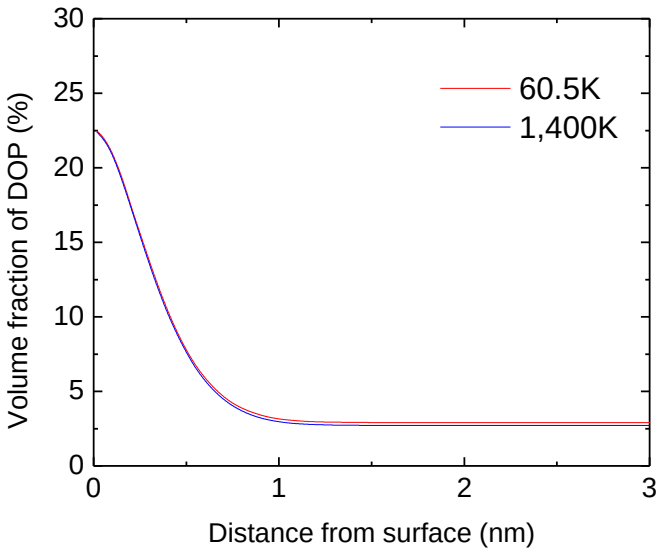

Fig. 4. Concentration of deuterated DOP (dDOP) plotted versus distance from the free surface of dDOP-added PS films with M_w = 60.5 and 1,400 kg/mol.

M_w < 100 kg/mol regime, η_{eff} is dominated by the mobility in the near surface region, M_{mobile}, as inferred from the same $\sim M_w^{3.2 \pm 0.2}$ scaling displayed by the data. The fitted

value of M_{mobile} of the plasticized films is about ~5 times that of the neat films. By using a compressible lattice model, Hariharan et al.[51] showed that the lower M_w species in a binary polymer mixture may preferentially partition to the free surface because such a partition increases entropy. Moreover, this effect can dominate even in cases where the surface tension of the lower M_w species is higher.[52, 53] To examine if the DOP in our films preferentially partitions to the free surface, we studied the concentration profile of dDOP (deuterated DOP) in dDOP-added PS-SiOx films with M_w = 60.5 and 1,400 kg/mol (h_0 = 11 and 13 nm, respectively) by using neutron reflectivity. The result is shown in Figure 4. As one can see, the profiles are essentially the same. According to these data, within 1 nm of the free surface the dDOP concentration decreases rapidly from ~22.5 vol% toward a constant level of ~3 vol%, which is consistent with the concentration of dDOP used to make the films (i.e., ~4.5 vol%) and the surface enrichments of dDOP being found (Figures 4 and S1). In the following, we estimate if the noted enrichment of dDOP at the free surface can account for the observed value of $M_{mobile,}$ i.e., $5 \times a_{mobile} M_w^{-3.2}$. Assuming the surface layer thickness, h_{mobile}, to be 1 nm (due to the data of Figure 4), one estimates that the surface layer viscosity, $\eta_{mobile} = h_{mobile}^3/(3M_{mobile})$,[13] is ($1.67 \times 10^{-11}$ Pa s g$^{-3.2}$ mol$^{3.2}$) $M_w^{3.2}$. Comparing this value to the data of the 4 wt% DOP added bulk PS taken at 120 ^oC (Figure 2), we find $\eta_{mobile}/\eta_{bulk} \approx$ 1/600 in the DOP-added films. We examine whether the observed surface enrichment of DOP may account for this value. To this end, we apply the free volume theory as we did before. We estimate that an addition of ~20 vol% DOP to a homopolymer should cause the viscosity to decrease by a factor of ≈ 1/60 = 1/ (17 × 3.5) and so a factor of ≈ 1/17 times that of the 4 wt% DOP-added bulk PS. Based on these estimates, the observed

M_{mobile} is ≈ 600 / 17 = 35 times larger than what the measured surface enrichment of DOP alone can account for. It follows that there should be enhanced surface mobility at the surface of PS enriched with ~20 vol% DOP, similar to that found in the surface of neat PS.

We now turn to the data of the DOP-added films with M_w > ~100 kg/mol in Figure 3. As discussed above, the data of the neat films in this M_w regime is consistent with M_{tot} being dominated by interfacial slippage. In eq 4, interfacial slippage is accounted for by the term, h_0^2/ξ. Because the interfacial friction coefficient ξ is an intensive parameter, this term and hence η_{eff} is not expected to exhibit any M_w dependence. On the other hand, the η_{eff} measurement of the DOP-added films clearly increases with increasing M_w in this region. One possible explanation is that the interfacial friction increases with M_w in these films. To explore this possibility, we studied the thickness of the irreversibly adsorbed layer that remains on the SiOx substrate after thin films of 4 wt% DOP-added PS films with an initial thickness of 200 nm are annealed at 150 ^oC for 80 h and then rigorously rinsed by toluene. A previous experiment [37] by us showed that the thickness of the irreversibly adsorbed layer, $h_{residue}$, is proportional to R_g, and the ratio $h_{residue}/R_g$ increases with the polymer-substrate interaction. Figure 5 (solid symbols) displays the result of $h_{residue}/R_g$ as a function of M_w. As seen, $h_{residue}/R_g$ increases with increasing M_w. This is consistent with the proposition made above that the polymer-substrate interaction of the DOP-added PS-SiOx increases with M_w. We surmise that this variation may arise from the local DOP concentration *immediate to* the SiOx substrate being not constant, but

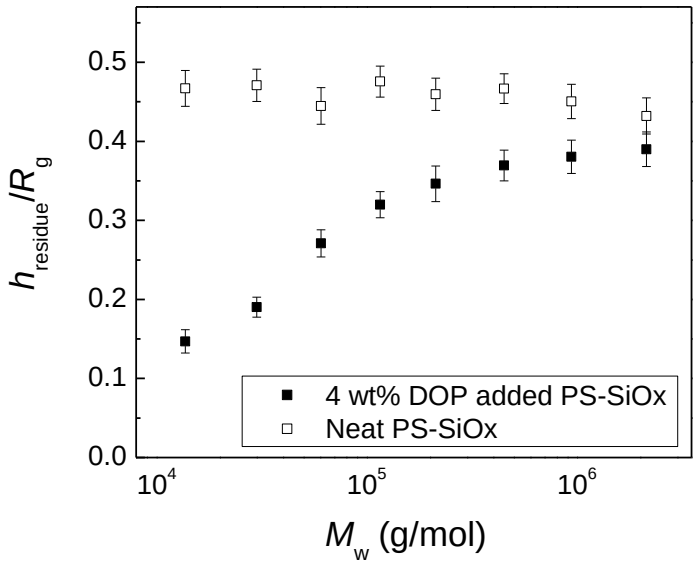

Fig. 5. Normalized irreversibly adsorbed film thickness, $h_{residue}$, of the 4wt%DOP-added and neat PS-SiOx films. The data are normalized by the R_g of the respective homopolymer and plotted as a function of M_w.

decreasing with M_w. We further suppose that this trend was shaped when the films were spin-coated from their solutions. Frantz and Granick [7] demonstrated that when a polymer solution is in contact with a solid substrate, the polymers adsorb quickly onto the substrate surface and at first sink into flattened conformations with almost 50% of the segments bonded to the surface. Chains that adsorbed later, finding fewer surface sites available then become attached by fewer segments. Although anchoring of the flattened chains occurs in the very initial times of spin-coating, considering the large number of chain segments per chain bound to the surface we believe that their flattened conformations remain in the final form of the spin-coated film and persist even with prolonged annealing above the T_g. This picture gains support from a recent finding of the

Koga group, [54] which shows that the irreversibly adsorbed layers formed in spin-coated PS-Si films upon extensive annealing are composed of a high-density inner flattened nanometer thick layer and a more tenuous outer layer. For PS absorbing onto silica from a good solvent, Linden et al. showed that the amount of polymer absorbed increases with M_w.[55] This is expected since longer polymer chains suffer less entropy loss upon adsorption.[56] Applying the same physics to a solution of PS and DOP, the concentration of DOP immediate to the substrate surface should decrease with increasing M_w.

To reconcile all our observations, we find it necessary to distinguish the DOP segregation effect just discussed, namely one that occurs during spin-coating while the film is in the solution state, from that occurs after the film dries and is thermally annealed. The second segregation process is well studied [56] and known to cause the lower M_w species of the film to partition to the substrate besides the free surface as discussed above, unless enthalpic effect happens to balance entropic effect. [57] Partition of dDOP to the substrate surface is also noticed here (Figures S1). If the DOP that partitions toward the substrate in the later process is unable to displace the chain segments that are already adsorbed on the substrate surface in the first process, the concentration of DOP immediate to the substrate surface and thereby the polymer-substrate interactions may not be affected by any DOP that arrives later. In view of the stability deliberated above of the initial adsorbed layer, this scenario is probable.

To assess whether the initial adsorbed polymer layer formed during spin-coating can dictate the subsequent interfacial properties of a film, we expose clean SiOx substrates to a 30 wt% solution of DOP in toluene before depositing the DOP-added PS-SiOx films and subjecting it to thermal annealing. We find that such "DOP treated"

substrates harbor a noticeably thinner irreversibly adsorbed layer with an average thickness that increases mildly from $(0.14 \pm 0.01) \times R_g$ to $(0.24 \pm 0.01) \times R_g$ as M_w is increased from 13.7 to 2,100 kg/mol. Our irreversibly adsorbed layer result thus supports the proposition that the final polymer-substrate interfacial properties of a film may be conditioned as early as when the film is first cast by spin-coating. Evoking our earlier observation [37] that bigger $h_{residue}/R_g$ corroborates with stronger polymer-substrate interactions and so the friction should be bigger, and further noting that the $h_{residue}/R_g$ ratio of the DOP-added films approaches that of the neat films at M_w = 2,100 kg/mol, one may qualitatively account for the difference found between the η_{eff} data of the neat and DOP-added films in the high M_w regime in Figure 3. Specifically, our observations suggest that it is caused by the combined effects of M_{tot} being dominated by interfacial slippage in the high M_w regime and the interfacial friction being increasing with M_w.

In the above, we have alluded to the presence of a confinement effect that helps promote interfacial slippage in the high M_w regime. To demonstrate this effect, we

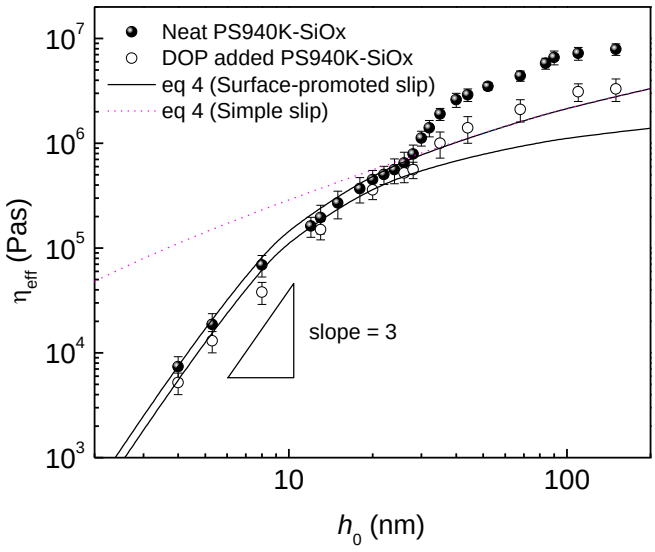

Fig. 6. Effective viscosity versus film thickness of PS neat films and DOP-added PS films supported by oxide coated silicon where the polymer M_W is 940 kg/mol. Data were taken at 182 ^oC. The solid lines are model lines obtained by using eqs 4 and 5 and the parameters displayed in Table 2. The dotted line is a model line using the same parameters except for α, which was set equal to 0.

display in Figure 6 the η_{eff} measurement of neat (solid symbols) and DOP-added PS-SiOx films (open symbols) with a M_w of 940 kg/mol plotted as a function of film thickness h_0. As seen, the η_{eff} of both kinds of films first increases with h_0 according to ~h_0^3. Then the growth slows down when h_0 exceeds ~10 nm. On reaching $h_0 \approx 28$ nm, close to the R_g of the polymer (~26 nm),[58] η_{eff} displays an abrupt jump before resuming a steady growth toward the bulk viscosity of ~2×10^7 Pa s. [44] Recall that our η_{eff} vs. M_w data of Figure 3, demonstrating M_w independence of η_{eff} for M_w > ~100 kg/mol, supports the proposition that interfacial slippage dominates the effect of enhanced surface mobility

in the high M_w domain. This corroborates with our finding that the slippage term, h_0^2/ξ, in eq 4 dominates M_{tot} therein. Using the definition, $\eta_{eff} \equiv h_0^3/(3M_{tot})$, it predicts that if ξ is a constant then $\eta_{eff} \sim h_0$, which departs from the empirical $\eta_{eff} \sim h_0^3$ dependence noted above. To make it easier to visualize that a constant ξ does not fit the data, we include in Figure 6 a model line (dotted line) that is obtained by putting ξ equal to a constant value of $(9.1 \pm 1.0) \times 10^{13}$ Nsm^{-3}. This choice of ξ brings agreement between the model and the neat film data just before the data jumps. The reason for this choice will become apparent later. Clearly, this line disagrees with the data in the thin film regime. It follows that a confinement effect that causes the friction coefficient ξ of the ultrathin films (referring here to those with $h_0 < \sim R_g$ films) to decrease with decreasing film thickness must be present. A recent analogous measurement on neat PS-SiOx films with other high M_w's (115 and 450 kg/mol) showed that the $\eta_{eff}(h_0/R_g)$ dependence of the ultrathin films and occurrence of a jump near $h_0 = R_g$ are common. [31] Taken together, our observations suggest that the envisaged confinement effect should bring about the empirical $\eta_{eff} \sim h_0^3$ dependence among the ultrathing films, but the effectiveness of this effect weakens drastically when h_0 exceeds R_g. We contemplate that for ultrathin films where $h_0 < \sim R_g$ the connection between the substrate surface and the free surface afforded by chain connectivity may help agitate the chain segments adherent to the substrate surface and thereby reduce friction. The idea that enhanced surface mobility may travel to the inner region of a polymer film through chain connectivity was first proposed by de Gennes.[59]

To model such a confinement effect on ξ, we observe that enhanced surface mobility causes M_{tot} to be enlarged by a multiplicative factor of $1+\frac{M_{mobile}}{h_0^3/(3\eta_{bulk})}$. We contemplate a similar enlargement factor for ξ^{-1}. To allow for variations, we introduce a constant parameter α as follows: [31]

$$\xi^{-1} = \left[1+\alpha\frac{M_{mobile}}{h_0^3/(3\eta_{bulk})}\right]\xi_0^{-1}, \qquad (5)\ (6)$$

where α is of the order unity. Recall that the value of ξ found by fitting the neat film data of Figure 3 is $(3.1 \pm 1.0) \times 10^{16}$ Nsm^{-3}. By substituting in eq 5 the values of ξ_0 and M_{mobile} found in Ref. [31] and the published values of η_{bulk},[44] we infer that $\alpha = 3.8 \pm 0.5$, which agrees within uncertainty with the value obtained before, [31] as expected.

Next, we fit our model (namely eq 4 with ξ given by eq 5) to the neat and DOP-added films in Figure 6. The fitted lines are displayed by the solid lines. As one can see, for $h_0 < R_g$, the model describes the data quite well. But for the thicker films, the model underestimates η_{eff}, which however may be anticipated if the proposed confinement effect (namely surface promoted slippage) originates from chain connectivity. The model parameters used to obtain the fitted lines in Figure 6 are shown in Table 2. In fitting the data, only M_{mobile} and ξ_0 are allowed to vary. The values of the other parameters are based on experimental or published values as specified in the footnote of Table 2. We find that the value of ξ_0 is almost exclusively determined by the η_{eff} measurement of the films just before it displays the jump near $h_0 \approx R_g$ (Figure 6). This may be evident from the onset of the convergence seen between the solid line and the dotted line around there.

(Recall that $M_{tot} \approx h_0^{\,2}\xi_0^{\,-1}\left[1+\alpha\frac{M_{\text{mobile}}}{h_0^3/(3\eta_{\text{bulk}})}\right]^{-1}$ in the $h_0 < \sim R_g$ thin film regime. So, the dotted line, corresponding to $\alpha = 0$, must agree with the general case corresponding to $\alpha \neq 0$ in the thick film limit, where $h_0^{\,3}/(3\eta_{\text{bulk}}) >> M_{\text{mobile}}$.) It may seem that one can alternatively opt to adjust the value of ξ_0 to match the η_{eff} data after the jump rather than before it as we opt to do here. But as we now discuss, this choice is not sound. Specifically, when we adjusted the value of ξ_0 to enforce a good fit of the model to the data after the jump, we found that the model always exhibits disagreement with the data just before the jump. But disagreement with the data before h_0 exceeds R_g is not expected since the model should be valid as long as chain connectivity is able to sustain surface-promoted slippage. Another shortcoming with the new fitting scheme is that we found the fitted values of ξ_0 of the neat and DOP added films to become different by a factor of ~10. But this is inconsistent with the above observation that h_{residue} of the two systems are similar (Figure 5). On the other hand, by enforcing a good fit before the jump, similar values of ξ_0 are obtained for the two systems as seen in Table 2.

Table 2. Model parameters used to produce the solid lines in Figure 6

	Neat PS940-SiOx	DOP-added PS940-SiOx
η_{bulk} (Pa s)	7.5×10^{6} a)	$7.5 \times 10^{6} / 4$ b)
α	3.8 ± 0.5 c)	3.8 ± 0.5 c)
M_{mobile} (m^3 Pa s^{-1})	$(1.1 \pm 1.0) \times 10^{-32}$ d)	$(1.1 \pm 1.0) \times 10^{-32} \times 5$ e)
ξ_0 (Nsm^{-3})	$(9.1 \pm 1.0) \times 10^{13}$ d)	$(8.3 \pm 1.0) \times 10^{13}$ d)

a) This value is based on the bulk viscosity data published in Ref. [44]

b) This value is slaved to the η_{bulk} value of the neat film divided by 4. The reduction factor of ¼ is based on the above finding that η_{bulk}(neat PS) / η_{bulk}(DOP-added PS) = 4.0 ± 0.5.

c) This is based on the value of α obtained above.

d) These are fitted values.

e) This value is slaved to the M_{mobile} value of the neat film multiplied by 5. The multiplying factor of 5 is based on the data of Figure 3 in the low-M_w regime.

CONCLUSION

We have examined the effects of nano-confinement on the effective viscosity, η_{eff}, of PS films plasticized by 4 wt% DOP and deposited on silica. Our results show that

nano-confinement may accentuate the effect of preferential segregation of DOP to the free surface or the substrate surface according to whether the polymer M_w is below or above ~100 kg/mol, respectively. For M_w below ~100 kg/mol, the η_{eff} of the plasticized films are uniformly decreased by a factor of ~5 relative to the neat films. While our result is consistent with our previous experiment (Ref. [31]) that in this low M_w regime the η_{eff} of nano-confined polymer films are dominated by the local mobility of a thin surface mobile layer at the free surface, an estimate based on the free volume theory showed that the observed enrichment of DOP therein alone may not account for the ~5 times reduction in the η_{eff} of the plasticized films noted above. An analogous mechanism that brings about enhanced mobility in the neat films may also be present in the plasticized films. For the higher M_w films, the η_{eff} of the plasticized films increases steadily toward that of the neat films as M_w is increased to 2,100 kg/mol. Such a change in η_{eff} toward independence of the added plasticizer indicates that the mechanism governing the flow dynamics switches to one that is less reliant on the plasticizer content with increasing M_w in the high-M_w regime. This observation is in good accord with the proposition we introduced in Ref. [31] that η_{eff} becomes dominated by surface-promoted interfacial slippage at high M_w. Further support of this proposition is found when we implement both enhanced surface mobility and surface-promoted interfacial slippage into eqs 4 and 5 and are able to apply these equations to obtain good description of the data, while maintaining consistency between all experimental observations and model assumptions.

ASSOCIATED CONTENT

Supporting Information

Figures S1 and S2. The Supporting Information is available free of charge on the ACS Publications website at DOI: 10.1021/acs.macromol.XXXXXXX.

AUTHOR INFORMATION

Corresponding Authors

*Email okctsui@bu.edu (O.K.C.T.).

*Email C.H.Lam@polyu.edu.hk (C.-H.L.).

Notes

The authors declare no competing financial interest.

ACKNOWLEDGMENTS

We are indebted to Prof. Catherine Klapperich for allowing us to use the vacuum press in her lab. O. K. C. T. is grateful to the support of the National Science Foundation through the projects DMR-1310536. C.H.L. thanks the support of Hong Kong GRF (Grant No. 15301014). The neutron reflectivity experiments were approved by the Neutron Scattering Program Advisory Committee of IMSS, KEK, Japan (Proposal No. 2009S08, 2009S14, 2015A0217, and 2015A0238).

REFERENCES

1. McKenna, G. B. *Eur. Phys. J. Special Topics* **2010,** 189, 285-302.

2. Ediger, M. D.; Forrest, J. A. *Macromolecules* **2014,** 47, 471-478.

3. Keddie, J. L.; Jones, R. A. L.; Cory, R. A. *Farad. Discuss.* **1994,** 98, 219-230.

4. Tsui, O. K. C.; Russell, T. P.; Hawker, C. J. *Macromolecules* **2001,** 34, 5535-5539.

5. Mundra, M. K.; Ellison, C. J.; Rittigstein, P.; Torkelson, J. M. *Eur. Phys. J. Special Topics* **2007,** 141, 143-151.

6. Li, R. N.; Chen, F.; Lam, C.-H.; Tsui, O. K. C. *Macromolecules* **2013,** 46, 7889-7893.

7. Frantz, P.; Granick, S. *Macromolecs* **1995,** 28, 6915-6925.

8. Ellison, C. J.; Mundra, M. K.; Torkelson, J. M. *Macromolecules* **2005,** 38, 1767-1778.

9. Ellison, C. J.; Ruszkowski, R. L.; Fredin, N. J.; Torkelson, J. M. *Phys. Rev. Lett.* **2005,** 92, 095702.

10. Tsui, O. K. C.; Zhang, H. F. *Macromolecules* **2001,** 34, 9139-9142.

11. Tanaka, K.; Takahara, A.; Kajiyama, T. *Macromolecules* **1997,** 30, 6626-6632.

12. Fakhraai, Z.; Forrest, J. A. *Science* **2008,** 319, 600-604.

13. Yang, Z.; Fujii, Y.; Lee, F. K.; Lam, C.-H.; Tsui, O. K. C. *Science* **2010,** 328, 1676-1679.

14. Paeng, K.; Swallen, S. F.; Ediger, M. D. *J. Am. Chem. Soc.* **2011,** 133, 8444-8447.

15. Peter, S.; Meyer, H.; Baschnagel, J. *Journal of Polymer Science: Part B: Polymer Physics* **2006,** 44, 2951-2967.

16. Starr, F. W.; Schroder, T. B.; Glotzer, S. C. *Phys. Rev. E* **2001,** 64, 021802.

17. Long, D.; Lequeux, F. *Eur. Phys. J. E* **2001,** 4, 371-387.

18. Herminghaus, S. *Eur. Phys. J. E* **2002,** 8, 237-243.

19. Mirigian, S.; Schweizer, K. S. *J. Chem. Phys.* **2014,** 141, 161103.

20. Lipson, J. E. G.; Milner, S. T. *Macromolecules* **2010,** 43, 9874-9880.

21. Hanakata, P. Z.; Douglas, J. F.; Starr, F. W. *Nat. Commun.* **2014,** 5, 4163.

22. Napolitano, S.; Wubbenhorst, M. *Nat. Commun.* **2011,** 2, 260.

23. Napolitano, S.; Rotella, C.; Wubbenhorst, M. *ACS Macro Lett.* **2012,** 1, 1189-1193.

24. Roth, C. B.; McNerny, K. L.; Jager, W. F.; Torkelson, J. M. *Macromolecules* **2007,** 40, 2568-2574.

25. Tito, N. B.; Lipson, J. E. G.; Milner, S. T. *Soft Matter* **2013,** 9, 9403-9413.

26. Kim, S.; Mundra, M. K.; Roth, C. B.; Torkelson, J. M. *Macromolecs* **2010,** 43, 5158-5161.

27. Ellison, C. J.; Torkelson, M. *Nature Mater.* **2003,** 2, 695-670.

28. Nguyen, H. K.; Labardi, M.; Lucchesi, M.; Rolla, P.; Prevosto, D. *Macromolecs* **2013,** 46, 555-561.

29. O'Connell, P. A.; Hutcheson, S. A.; McKenna, G. B. *J. Polym. Sci. B: Polym. Phys.* **2008,** 46, 1952-1965.

30. Serghei, A.; Kremer, F. *Macromol. Chem. Phys.* **2008,** 209, 810-817.

31. Chen, F.; Peng, D.; Lam, C.-H.; Tsui, O. K. C. *Macromolecules* **2015,** 48, 5034-5039.

32. Ye, X.-Y.; Lin, F.-W.; Huang, X.-J.; Lian, H.-Q.; Xu, Z.-K. *RSC Advances* **2013,** 3, 13851-13858.

33. Brandrup, J.; Immergut, E. H., *Polymer Handbook*. 3 ed.; Wiley: New York, 1989.

34. Savin, D. A.; Larson, A. M.; Lodge, T. P. *J. Polym. Sci. B: Polym. Phys.* **2004,** 42, 1155-1163.

35. Yamada, N. L.; Torikai, N.; Mitamura, K.; Sagehashi, H.; Sato, S.; Seta, H.; Sugita, T.; Goko, S.; Furusaka, M.; Oda, T.; Hino, M.; Fujiwara, T.; Takahasi, H.; Takahara, A. *Euro. Phys. J. Plus* **2011,** 126, 108.

36. Mitamura, K.; Yamada, N. L.; Sagehashi, H.; Torikai, N.; Arita, H.; Terada, M.; Kobayashi, M.; Sato, S.; Seto, H.; Goko, S.; Furusaka, M.; Oda, T.; Hino, M.; Jinnai, H.; Takahara, A. *Polym. J.* **2013,** 45, 100-108.

37. Fujii, Y.; Yang, Z.; Leach, J.; Atarashi, H.; Tanaka, K.; Tsui, O. K. C. *Macromolecules* **2009,** 42, 7418-7422.

38. Chen, F.; Lam, C.-H.; Tsui, O. K. C. *Science* **2014,** 343, 975.

39. Jiang, Z.; Mukhopadhyay, M. K.; Song, S.; Narayanan, S.; Lurio, L. B.; Kim, H.; Sinha, S. K. *Phys. Rev. Lett.* **2008,** 101, 246104.

40. Lam, C.-H.; Tsui, O. K. C.; Peng, D. *Langmuir* **2012,** 28, 10217-10222.

41. Fredrickson, G. H.; Ajdari, A.; Leibler, L.; Carton, J. P. *Macromolecules* **1992,** 25, (11), 2882-2889.

42. Zhao, H.; Wang, Y. J.; Tsui, O. K. C. *Langmuir* **2005,** 21, 5817-5824.

43. Fetters, L. J.; Lohse, D. J.; Milner, S. T. *Macromolecules* **1999,** 32, 6847-6851.

44. Majeste, J.-C.; Montfort, J.-P.; Allal, A.; Marin, G. *Rheo. Acta* **1998,** 37, 486-499.

45. Rubinstein, M.; Colby, R. H., *Polymer Physics*. Oxford University Press: New York, 2003.

46. Colby, R. H.; Fetters, L. J.; Funk, W. G.; Graessley, W. W. *Macromolecules* **1991,** 24, 3873-3882.

47. Doolittle, A. K. *J. Appl. Phys.* **1951,** 22, (12), 1471-1475.

48. Peng, D.; Li, R. N.; Lam, C.-H.; Tsui, O. K. C. *Chin. J. Polym. Sci.* **2013,** 31, 12-20.

49. Chai, Y.; Salez, T.; McGraw, J. D.; Benzaquen, M.; Dalnoki-Veress, K.; Raphael, E.; Forrest, J. A. *Science* **2013,** 343, 994.

50. Lam, C.-H.; Tsui, O. K. C. *Phys. Rev. E* **2013,** 88, (88), 042604.

51. Hariharan, A.; Kumar, S.; Russell, T. P. *J. Chem. Phys.* **1993,** 99, 4041-4050.

52. Hariharan, A.; Kumar, S. K.; Russell, T. P. *J. Chem. Phys.* **1993,** 96, 4163-4173.

53. Tanaka, K.; Kajiyama, T.; Takahara, A.; Tasaki, S. *Macromolecs* **2002,** 35, 4702-4706.

54. Jiang, N.; Shang, J.; Di, X.; Endoh, M. K.; Koga, T. *Macromolecules* **2014,** 27, 2682-2689.

55. Linden, C. V.; Leemput, R. V. *J. Colloid Interface Sci.* **1978,** 67, 48-62.

56. Cohen Stuart, M. A.; Fleer, G. J. *Annu. Rev. Mater. Sci.* **1996,** 26, 463-500.

57. Genzer, J.; Faldi, A.; Oslanec, R.; Composto, R. J. *Macromolecs* **1996,** 29, 5438-5445.

58. Fetters, L. J.; Lohse, D. J.; Witten, T. A.; Zirkel, A. *Macromolecules* **1994,** 27, 4639-4647.

59. De Gennes, P.-G. *Eur. Phys. J. E* **2000,** 2, 201-205.

Confinement Effect on the Effective Viscosity of Plasticized Polymer Films

F. Chen,[1] D. Peng,[1] Y. Ogata,[2] K. Tanaka,[2] Z. Yang,[3] Y. Fujii,[4] N. L. Yamada,[5] C. -H. Lam,[6*] and O. K. C. Tsui[1,7]*

[1]*Department of Physics, Boston University, Boston, MA 02215.*

[2]*Department of Applied Chemistry, Kyushu University, Fukuoka 819-0395, Japan*

[3] *Department of Polymer Science and Engineering, Soochow University, P. R. China*

[4] *National Institute for Materials Science, 1-1 Namiki, Tsukuba, Japan.*

[5] *Neutron Science Laboratory, High Energy Accelerator Research Organization, Ibaraki 305-0044, Japan.*

[6] *Department of Applied Physics, Hong Kong Polytechnic University, Hung Hom, Hong Kong.*

[7] *Division of Materials Science & Engineering, Boston University, Brookline, MA 02446.*